Bioresource Technology 354 (2022) 127222

Contents lists available at ScienceDirect

Bioresource Technology

journal homepage: www.elsevier.com/locate/biortech

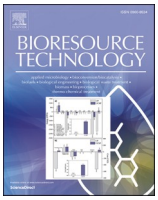

Metabolic pathways for biosynthesis and degradation of starch in *Tetraselmis chui* during nitrogen deprivation and recovery

Giorgia Carnovale [a,b], Carmen Lama [c], Sonia Torres [c], Filipa Rosa [a], Lalia Mantecón [c], Svein Jarle Horn [b], Kari Skjånes [a,*], Carlos Infante [c]

[a] Norwegian Institute of Bioeconomy Research (NIBIO), Division of Biotechnology and Plant Health, PO 115, NO−1431 Ås, Norway
[b] Norwegian University of Life Sciences (NMBU), Faculty of Chemistry, Biotechnology and Food Science, P.O. Box 5003, NO−1432 Ås, Norway
[c] Fitoplancton Marino, S.L., Dársena comercial s/n (Muelle pesquero), 11500 El Puerto de Santa María, Cádiz, Spain

HIGHLIGHTS

- *T. chui* efficiently accumulates up to 59% starch under nitrogen deprivation.
- Recovery from stress begins within 12 h after nutrient replenishment.
- Nitrogen deprivation has a strong impact on regulation of starch-related genes.
- Gene expression results challenge the traditional starch metabolism model.
- Post-transcriptional regulatory mechanisms seem to play a crucial role in *T. chui*.

ARTICLE INFO

Keywords:
Microalgae
Tetraselmis
Starch
Gene expression
Nitrogen

ABSTRACT

Tetraselmis chui is known to accumulate starch when subjected to stress. This phenomenon is widely studied for the purpose of industrial production and process development. Yet, knowledge about the metabolic pathways involved is still immature. Hence, in this study, transcription of 27 starch-related genes was monitored under nitrogen deprivation and resupply in 25 L tubular photobioreactors. *T. chui* proved to be an efficient starch producer under nitrogen deprivation, accumulating starch up to 56% of relative biomass content. The prolonged absence of nitrogen led to an overall down-regulation of the tested genes, in most instances maintained even after nitrogen replenishment when starch was actively degraded. These gene expression patterns suggest post-transcriptional regulatory mechanisms play a key role in *T. chui* under nutrient stress. Finally, the high productivity combined with an efficient recovery after nitrogen restitution makes this species a suitable candidate for industrial production of high-starch biomass.

1. Introduction

Starch is the primary storage compound in plants and an essential carbohydrate source for human and animal nutrition. Production of starch as a reserve in microalgal cells has been widely studied for its potential use as a feedstock for bioethanol and other biorefinery processes (Chowdhury and Loganathan, 2019; Zhang et al., 2021), but also for applications in human nutrition, due to its putative functional and structural properties (Gifuni et al., 2017; Shahid et al., 2020). Regulation of starch synthesis and degradation in microalgae is linked to the shift between optimal and suboptimal growth conditions and has been the subject of several studies (Ran et al., 2019; Shahid et al., 2020).

Species from the genus *Tetraselmis* are considered attractive for industrial production, having already been established as live feed in aquaculture of molluscs and shrimps and as an enrichment of other meals. Particularly, they are reported to have high specific growth rates (Reitan et al., 2021) and have shown to be high-starch producers under nutrient stress (Yao et al., 2018). A critical parameter for industrial production in semi-continuous modes is the recovery from nutrient-induced stressful conditions. In this regard, *Tetraselmis subcordiformis* has shown a speedy recovery from nutrient stress, with starch being degraded within 24 h after nutrient restitution (Yao et al., 2012). It is

* Corresponding author.
E-mail address: kari.skjanes@nibio.no (K. Skjånes).

https://doi.org/10.1016/j.biortech.2022.127222
Received 24 February 2022; Received in revised form 20 April 2022; Accepted 21 April 2022
Available online 25 April 2022

important to note that, within this genus, *Tetraselmis chui* is the only species that has been authorised for human consumption (since 2014) as a novel food in the European Union (EU) and, more recently (2017), also as a food supplement (Mantecón et al., 2019), widening the range of its possible industrial applications.

The traditional model of starch metabolic pathways in microalgae has been developed in the model organism *Chlamydomonas reinhardtii* (Ball and Deschamps, 2009; Busi et al., 2014), while an additional pathway map looking in depth at the fluxes of starch metabolism during day-night cycles was developed in *Ostreococcus tauri* (Sorokina et al., 2011). Both models identify the first regulatory step to be the phosphorylation of glucose-1-phosphate (Glc-1-P) to ADP-glucose by the ADP-glucose-pyrophosphorylase (AGPase). Different isoforms of starch synthases (SS) form crystalline starch using this basic building block. The granule-bound SS (GBSS) catalyses the formation of α(1–4) bonds, elongating existing glucan chains, and is strictly connected to the starch granules during metabolism. Short glucan chains are produced in the chloroplast lumen by soluble starch synthase isoforms (SSS). Starch branching enzymes (SBE) form amylopectin or branched glucans by transferring linear glucan chains to the carbon 6 of an existing chain within the granule. This process is further assisted by the isoamylase 1 (ISA1) and 2 (ISA2), which are suggested to cleave branches that are improperly positioned for the sake of crystallisation, releasing soluble oligosaccharides, and by the disproportionating enzyme (DPE), which alters the chain length of such oligosaccharides recycling them to substrates useful for SS and SBE.

Starch degradation back to Glc-1-P requires the glucan chains to be phosphorylated by water dikinases (WD). After that, beta- and alpha-amylases (AMB and AMA) hydrolyse α(1–4) glycosidic bonds, while debranching enzymes, such as isoamylase 3 (ISA3), hydrolyse the α(1–6) bonds. Both processes release glucan chains that contribute to the pool of available maltose oligosaccharides (MOS) and water-soluble polysaccharides (WSP), whose chain length may be modified again by the DPE. Starch phosphorylase (SPh) finally catalyses the formation of Glc-1-P, which is then readily available again as substrate for the Calvin cycle and other metabolic processes.

The intricate mechanisms involved in starch synthesis and degradation in microalgae are, however, not yet understood completely. In this regard, a recent body of literature has consistently challenged the traditional *C. reinhardtii* model on the role of some enzymes (Ran et al., 2019), with studies performed on several genes, enzymes and species. Hence there is a clear need for further in-depth studies to shed light on responses to stress and recovery, especially in species of high commercial interest.

The aim of this work was to perform a comprehensive analysis of starch biosynthesis and degradation mechanisms in *T. chui* subjected to nitrogen starvation and subsequent recovery at a pilot-scale. Thus, growth and biomass composition of *T. chui* cultivated in 25 L tubular photobioreactors were monitored throughout the trial. In an attempt to understand the molecular basis underlying starch metabolism, transcriptional regulation of 27 genes involved both in starch synthesis and degradation was furthermore analysed by RT-qPCR. Results obtained in this study will widen the existing knowledge about starch metabolism in this economically relevant species.

2. Materials and Methods

2.1. Algae cultivation

T. chui SAG 8–6 obtained from SAG Culture Collection of Algae (Göttingen, Germany) was grown on agar plates on L1 medium at 22 °C and irradiated with 20 μmol m^{-2} s^{-1} with LED lights. The algae were scaled up in 2xF 50–100 μmol m^{-2} s^{-1} on a shaking plate with 1% CO_2: air mixture first to 500 mL and then to 1 L Erlenmeyer flasks. The cultures were used first to inoculate a 25 L GemTube RD1-25, tubular photobioreactor (LGem BV, Netherlands) in 2xF medium and then for further scale-up in 250 L GemTube RD1 − 250 tubular photobioreactor (LGem BV, Netherlands). In the tubular reactors, temperature was set to 25 ± 3 °C maintained via a room-temperature control; surface irradiance was set to 100 μmol m^{-2} s^{-1} and pH was set to 7.8 ± 0.2, controlled by CO_2 addition. After three days, the inoculum was sourced from the running 250 L reactor taking a 5 L culture sample which was gently centrifuged for 5 min at 2500 rpm. The pellet was rinsed with the new growth medium and used to begin the experiment, inoculating two 25 L photobioreactors (PBR 1 and PBR 2) at the same initial density of 0.5 ± 0.06 × 10^6 cells ml^{-1}. The medium used upon inoculation was a modified 2xF medium which contained only half of the nitrogen concentration (1.78 mM) to induce stress and starch accumulation gradually. Light was set to 150 μmol m^{-2} s^{-1}, and after three days under nitrogen deprivation, all nutrient stocks were resupplied in non-limiting amounts (4xF medium) for the recovery phase of the experiment.

2.2. Cultivation monitoring

Algal growth was monitored daily by spectrophotometry, measuring absorbance at 750 nm with a SparkTM microplate reader (Tecan®, Switzerland). Data from the plate reader were converted to 1 cm cuvette light-path, with a calibration curve based on *T. chui* cultures.

Dry weight was assessed filtrating a known volume of culture, diluted in 20 mL 0.5 M ammonium formate, in pre-washed and -weighed Whatman GF/F glass fibre filters 25 mm diameter with 0.7 μm pore size (Cytiva, UK). Subsequently, filters were dried in a drying oven at 105 °C for 24–48 h before weighing.

Samples were stored in paraformaldehyde 2% for further analyses, and cell counts were performed using a Guava® easyCyte Flow Cytometer (Luminex Corporation, USA) with a minimum of 50,000 events screened per sample.

Quantum yield (*Fv/Fm*) was measured on the spot with Aquapen PAM fluorometer (Photon Systems Instruments, Czech Republic).

Nitrogen consumption was assessed on the spot using the colorimetric Nitrate Test strips, 10–500 mg L^{-1} (NO_3^-), MQuant® (Supelco). Values were later confirmed with ion chromatography performed with the 940 Professional IC Vario (Metrohm AG, Switzerland).

2.3. Biomass analysis

Biomass harvested at each timepoint was freeze-dried and then stored for analysis. For starch determination, 7 ± 1 mg were weighed in triplicates and exposed to bead − beating in ethanol to break the cell walls and remove interfering compounds. Starch was quantified using the Total Starch (AA/AMG) Assay Kit (Megazyme, Ireland). Protein content was analysed using 10 ± 1 mg freeze-dried biomass with the Bio-Rad protein assay dye reagent (Bio-Rad, USA) against a bovine serum albumin standard curve.

2.4. Total RNA isolation and cDNA synthesis

Cell lysis was performed in the Bullet Blender® 24 (Next Advance, USA) using 0.2 mm stainless steel beads (Next Advance) for 3 min and speed set at 10. The NucleoSpin® Plant II kit (Macherey-Nagel, Germany) was employed to isolate total RNA following the manufacturer's instructions. Removal of residual genomic DNA was ensured by treating twice all RNA samples with DNase I. RNA quantification was accomplished using the NanoDrop 2000 spectrophotometer (Thermo Scientific, USA), and appropriate quality was checked in agarose gels. The total RNA (1 μg) from each sample was reverse-transcribed using the iScript™ cDNA Synthesis kit (Bio-Rad, USA) in a reaction volume of 20 μL according to the manufacturer's protocol. Finally, a volume of 80 μL of nuclease-free water was added to each reaction (5-fold dilution). Two randomly selected samples were amplified by PCR, in absence of cDNA synthesis, to confirm the lack of genomic DNA contamination. Primer design and RT-qPCR.

For gene expression normalisation, the stability of up to six potential reference genes was evaluated (Table 1). They were selected based on previously reported data (Torres et al., 2021). For the target genes employed in this study, predicted coding sequences of close to 22,600 transcripts identified in the *T. chui* strain PLY429 were retrieved from the iMicrobe data set (https://www.imicrobe.us/) and then annotated using the AutoFACT tool (Koski et al., 2005). A total of 27 transcripts of interest were selected, and the predicted encoding polypeptides were obtained with EditSeq v8.1.3 (DNASTAR). After that, appropriate annotation was confirmed with BLASTp (Table 1). The presence of putative chloroplast signal peptides in the N-terminal portion of predicted polypeptide sequences (when non-truncated) was analysed using the bioinformatic tool TargetP 2.0 (Armenteros et al., 2019).

Primer pairs for the candidate reference genes and the target genes *AGPLs* and *AGPSs* were the same as previously reported (Torres et al., 2021). Primers for the remaining 25 target genes (See supplementary material) were designed using Oligo v7.60 software (Molecular Biology Insights). Appropriate performance of each primer pair was double-checked, first by PCR amplification of the target amplicons (using the same conditions described below for RT-qPCR) and then by loading the products in standard agarose gel electrophoresis. A single DNA band of the expected sizes was obtained in each instance (data not shown).

RT-qPCR was performed using a CFX96™ Real-Time PCR Detection System (Bio-Rad, USA). Reactions contained 5 μL of 2X iQ™ SYBR® Green Supermix (Bio-Rad, USA), 0.3 μL of forward and reverse primers (10 μM stock each; final concentration of 300 nM), 2 μL of cDNA (retrotranscribed from 20 ng of RNA), and 2.4 μL of nuclease-free water. Reactions were run in duplicate and for further calculations, the mean threshold cycle (C_T) was used.

Two different tools were used to select the most appropriate reference genes. The first one was geNorm (version 3.5), or pairwise comparison approach (Vandesompele et al., 2002), in which candidate genes are ranked according to their expression stability. The second software was NormFinder (version 0.953), in which the candidate reference genes are ranked using a model-based approach that ranks the candidate reference genes according to their minimal combined inter- and intra-group expression variation (Andersen et al., 2004). To generate valid input data files for both geNorm and NormFinder, raw C_T values were first exported to a Microsoft Excel sheet and then transformed into relative quantities using the comparative C_T method. To achieve this and for each candidate reference gene, the lowest C_T value was subtracted from all other C_T values, thus transforming C_T values into ΔC_T values. After that, the formula $2^{-\Delta Ct}$ was applied to each data point to obtain relative quantities. As the formats for presenting input data were different in geNorm and NormFinder, relative quantities calculated as previously described were exported into new Excel datasheets and converted according to the specific software requirements.

For each gene, relative transcript levels were determined using the $2^{-\Delta\Delta Ct}$ method (Livak and Schmittgen, 2001). The thermal cycling profile was as follows: incubation at 95 °C for 3 min, and then 40 × 15 s cycles at 95 °C and 68 °C for 30 s. For each primer pair, specificity was verified through a melting curve analysis from 70 °C to 95 °C, using a ramp speed of 0.5 °C every 10 s. In each instance, a single and sharp peak was obtained.

2.5. Statistical analysis of RT-qPCR data

Statistical analyses were conducted using Prism 6 (GraphPad Software) after normalisation with *RPS10* and *UBCE*. In all instances, the Kruskal-Wallis test (non-parametric one-way ANOVA) was applied and when significant, Dunn's multiple comparison test was performed. Significance was accepted for $p \leq 0.05$.

Table 1
List of reference and target genes in *Tetraselmis chui* and the respective primers used for RT-qPCR. (*) sequence retrieved from GenBank. (See supplementary material for primer sequences, Tm and amplicon length).

CANDIDATE REFERENCE GENES		
Gene	Sequence ID (*T. chui* strain PLY429)	Sequence ID (AutoFact + BLAST)
ACT	MMETSP0491_2-20121128|5070_1	Actin
EFL	MMETSP0491_2-20121128|385_1	Elongation factor-1 alpha like
cdkA	MMETSP0491_2-20121128|4820_1	Cell division control protein 2 homolog A isoform X1
rbcL	HF931099*	Chloroplast ribulose-1,5-bisphosphate carboxylase/oxygenase large subunit
UBCE	MMETSP0491_2-20121128|9783_1	Ubiquitin-conjugating enzyme
RPS10	MMETSP0491_2-20121128|7667_1	40S ribosomal protein S10
TARGET GENES		
Gene	Sequence ID (*T. chui* strain PLY429)	Sequence ID (AutoFact + BLAST)
AGPLs	MMETSP0491_2-20121128|23823_1	Glucose-1-phosphate adenylyltransferase large subunit
AGPSs	MMETSP0491_2-20121128|4141_1	Glucose-1-phosphate adenylyltransferase small subunit
GBSS1	MMETSP0491_2-20121128|5277_1	Granule-bound starch synthase
GBSS2	MMETSP0491_2-20121128|1231_1	Granule-bound starch synthase
SSS1	MMETSP0491_2-20121128|9227_1	Soluble starch synthase
SSS2	MMETSP0491_2-20121128|10712_1	Soluble starch synthase
SSS3	MMETSP0491_2-20121128|5181_1	Soluble starch synthase
SSS4	MMETSP0491_2-20121128|8254_1	Soluble starch synthase
SSS5	MMETSP0491_2-20121128|5721_1	Soluble starch synthase
SBE1	MMETSP0491_2-20121128|5189_1	Starch branching enzyme
SBE2	MMETSP0491_2-20121128|6860_1	Starch branching enzyme
AMA1	MMETSP0491_2-20121128|7949_1	Alpha amylase
AMA2	MMETSP0491_2-20121128|21071_1	Alpha amylase
AMA3	MMETSP0491_2-20121128|15281_1	Alpha amylase
AMA4	MMETSP0491_2-20121128|10987_1	Alpha amylase
AMA5	MMETSP0491_2-20121128|11752_1	Alpha amylase
AMB1	MMETSP0491_2-20121128|2795_1	Beta amylase
AMB2	MMETSP0491_2-20121128|4712_1	Beta amylase
AMB3	MMETSP0491_2-20121128|22759_1	Beta amylase
DPE	MMETSP0491_2-20121128|19976_1	Disproportionating enzyme
SPh	MMETSP0491_2-20121128|6575_1	Starch phosphorilase
ISA1	MMETSP0491_2-20121128|9150_1	Isoamylase 1
ISA3	MMETSP0491_2-20121128|11209_1	Isoamylase 3
PWD	MMETSP0491_2-20121128|4718_1	Phosphoglucan water dikinase
GWD	MMETSP0491_2-20121128|3077_1	Alpha-glucan water dikinase
DBE1	MMETSP0491_2-20121128|24193_1	Starch debranching enzyme (Limit dextrinase)

(*continued on next page*)

Table 1 (*continued*)

TARGET GENES		
Gene	Sequence ID (*T. chui* strain PLY429)	Sequence ID (AutoFact + BLAST)
DBE2	MMETSP0491_2-20121128|26458_1	Starch debranching enzyme (Alpha-1,6 glucosidase, pullulanase-type)

3. Results and discussion

3.1. Algal cultivation

In this study, *T. chui* growth was monitored during two phases. First, cultures were inoculated in a modified 2xF medium containing a reduced nitrate content, equivalent to the proportion present in standard F medium (1.78 mM), to induce starch accumulation. Second, after the starch content reached values above 30% of the dry weight, nutrient stock solutions were resupplied in non-limiting concentrations (equivalent to 4xF medium) to examine how the cultures would recover.

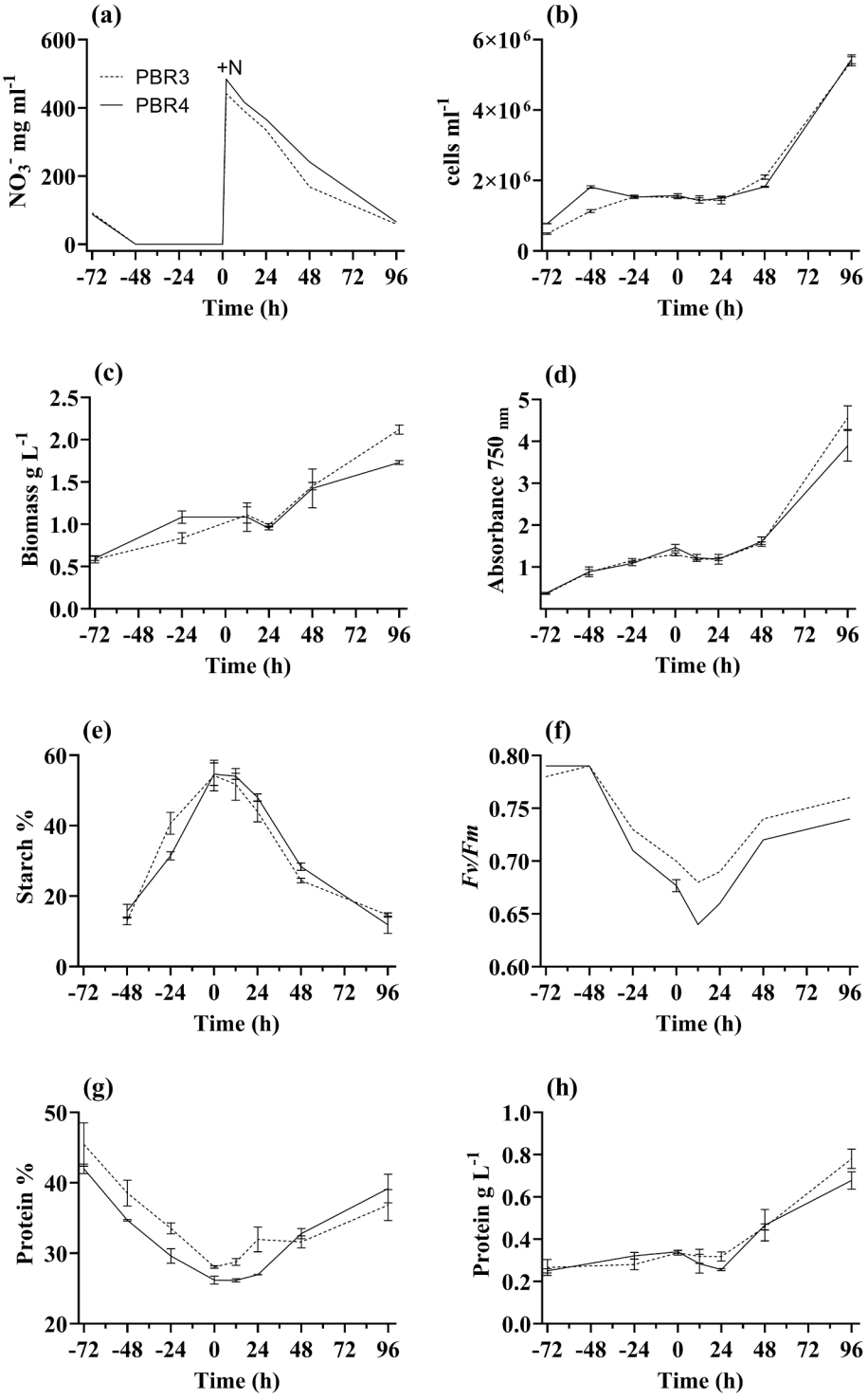

Fig. 1. Time course of cell growth and biomass changes in *Tetraselmis chui* in two parallel 25 L tubular photobioreactors, PBR 1 (dotted line) and PBR 2 (solid line). Timepoint 0 on the × axis corresponds to the moment of nitrogen replenishment. (a) flow cytometry cell counts; (b) nitrate concentration in culture medium; (c) biomass dry weight; (d) absorbance at 750 nm; (e) starch concentration expressed as % of biomass dry weight; (f) quantum yield; (g) protein concentration expressed as % of biomass dry weight; (h) protein concentration expressed as grams per litre.

The use of a reduced nitrogen content at inoculation was preferred over immediate and complete starvation. It has been previously shown that this approach induces a higher starch accumulation and better productivity, possibly due to the milder and more gradual advent of stressful conditions (Yao et al., 2017). The nitrogen supplied was consumed within the first 24 h (Fig. 1a), resulting in halted culture growth with no further increase in cell numbers (Fig. 1b). However, a slight increase in dry weight (Fig. 1c) and absorbance at 750 nm (Fig. 1d) were observed, due to storage compound accumulation and changes in cell granularity. After nitrogen restitution at high concentration, all growth parameters showed signs of recovery within 48 h.

In the pilot-scale set-up assessed in this work, nitrogen starvation led to a 3.5-fold increase in the relative starch content (Fig. 1e), reaching 58.5% ± 2 of the biomass dry weight. Species from the genus *Tetraselmis* are known to produce such high storage contents at lab-scale, and up to 62% of starch has been previously found (Yao et al., 2012). During the replenishment phase, starch degradation started after 12 h. The decrease proceeded slowly to reach 25% of starch content within 48 h and finally returned to basal level after 96 h.

Nitrogen is a primary constituent of proteins, and its absence results in reduced cell functions and protein synthesis. In the first phase, as expected, relative protein content in the biomass decreased concomitantly to an increase in starch reserves, whereas the protein content in the cultures (expressed as g L^{-1}) was halted (Fig. 1 g-h). In the second phase, recovery started after 24 h from replenishment, in parallel with cell division. Overall, a very similar performance of the two parallel 25 L reactors could be observed (Fig. 1).

Photosynthetic activity has also proved essential for starch metabolism during stress conditions (Carnovale et al., 2021; Janssen et al., 2018; Li et al., 2015). Therefore, it becomes crucial to ensure that the cultures are not limited or inhibited by light and receive an adequate irradiance dose. Quantum yield (*Fv/Fm*) has been studied as a proxy for the activity of Photosystem II, in combination with stress-induced starch accumulation. Its threshold for efficient starch production has been identified to be above 0.60 for both *Chlorella vulgaris* (Brányiková et al., 2011) and *T. subcordiformis* (Yao et al., 2012). In this study *Fv/Fm* decreased after nitrogen consumption from 0.79 ± 0.01 to 0.68 ± 0.03 (Fig. 1f). Such values did nonetheless not hinder starch accumulation. Quantum yield further decreased after nitrogen resupply. However, it recovered faster than other parameters monitored, with values returning to levels above 0.70 within 48 h.

Former studies on phosphorus deprivation in *T. subcordiformis* have shown a faster recovery from stress (Yao et al., 2012). Thus, it could be hypothesised that nitrogen deprivation has a more substantial impact on cell metabolism. It is noteworthy that in the pilot-scale experiment nutrient replenishment did not directly result in significant changes in culture density over 48 h.

3.2. Selection of candidate reference genes for RT-qPCR

Gene expression analysis by quantitative real-time reverse transcription PCR (RT-qPCR) is considered a valid and commonly used tool to provide information concerning molecular regulatory mechanisms associated to cellular processes owing to its speed, high sensitivity, cost, accuracy, reliability and reproducibility (Gao et al., 2020; Mou et al., 2015). However, appropriate selection of reference genes is crucial in order to normalise RT-qPCR thus minimising the effect of potential interfering factors. Hence, stability of candidate reference genes has to be validated under specific experimental conditions as expression profiles are not always constant (Chapman and Waldenström, 2015; Radonić et al., 2004). With this aim, different mathematical algorithms have been developed to evaluate the suitability of reference genes, with geNorm (Vandesompele et al., 2002) and NormFinder (Andersen et al., 2004) among the most widely employed tools. As an appropriate selection of stable genes is a major factor to ensure gene expression data reliability, a high number of studies have been conducted in different organisms and cell types, including microalgae (Cao et al., 2012; Guo et al., 2013; Liu et al., 2020). Particularly, the expression stability of up to 18 different candidate reference genes has been recently evaluated in the green microalgae *T. chui* using samples collected from large scale industrial photobioreactors and indoor cultures (Torres et al., 2021). Taking advantage of the results obtained in that previous report, a set of six genes that were revealed to be highly stable (*RPS10*, *EFL*, *ACT*, *rbcL*, *UBCE* and *cdkA*; see Table 1) were selected to check suitability as reference genes using geNorm and NormFinder in samples collected in this study.

First, the average expression stability (M) values of the six candidate reference genes were determined using the geNorm algorithm (Fig. 2a). All the genes exhibited an M value below the 1.5 geNorm threshold. The most stable genes across timepoints were *UBCE/cdkA*, followed by *RPS10*. Next, pairwise variation values (V) were calculated with a cut-off suitability set at 0.15 (Fig. 2b) to identify the ideal number of reference genes needed for accurate expression normalisation. The combination of two genes rendered this value of 0.15, but the addition of more genes revealed to increase V. Thus, only two genes were used for normalisation. Stability was also evaluated using the NormFinder software (Fig. 2c). In line with geNorm, the most stable genes were *RPS10*, *UBCE* and *cdkA*. Given the known sensitivity of geNorm to co-expressed genes, *RPS10* (the most stable gene in NormFinder) and *UBCE* (one of the two most stable genes with geNorm, and the second most stable gene with NormFinder) were finally selected for gene expression normalisation. Results obtained in this work are in agreement with those previously reported in a comprehensive ranking of 18 potential reference genes in *T. chui*, showing *RPS10* and *UBCE* among the four most stable genes (Torres et al., 2021).

3.3. Expression of target genes

Quantitative analysis of gene expression is undoubtedly a powerful tool in order to unravel the molecular and biochemical events that underlie physiological characteristics and responses to environmental changes in any given organism. Fortunately, genetic resources have been exponentially increasing during the last decade thanks to Next Generation Sequencing technologies, and thus complete genomes as well as transcriptomes obtained by RNA sequencing (RNA-Seq) of many different organisms and cell types are nowadays available in databases. Regarding microalgae, this last high throughput technology has been applied with success to analyse the whole adaptive physiological responses to changes in varying culture conditions (Corteggiani Carpinelli et al., 2014; Scarsini et al., 2022). However, to study particular metabolic pathways, the construction of RT-qPCR platforms for the expression analysis of a variable number of selected and representative genes becomes a valuable approach. In this regard and owing to the reliability and accuracy of RT-qPCR, this strategy has been followed, for instance, to validate RNA-seq data in the green microalgae species *Chlorella sorokiniana* (Li et al., 2016), *Tetraselmis* sp. M8 (Lim et al., 2017) and *Tetraselmis suecica* (Lauritano et al., 2019). Moreover, the influence of light quality on metabolism has been studied using a RT-qPCR platform containing more than 100 selected genes in the Eustigmatophyceae *Nannochloropsis gaditana* (Patelou et al., 2020). These studies highlighted how gene expression analysis of selected markers by RT-qPCR can be used in microalgae to study the modulation of metabolic pathways in response to environmental changes. In the present study, availability of a full *T. chui* transcriptome (strain PLY429; see Materials and Methods) allowed identification of a set of 27 genes (Table 1) potentially involved in starch biosynthesis and degradation (Busi et al., 2014). Thus, primer pairs could be designed to create a specific RT-qPCR platform to study starch metabolism during nitrogen deprivation and further recovery.

Gene expression results had a low variation between the two parallel culture units. As a whole, expression patterns in *T. chui* during nitrogen deprivation showed an overall down-regulation of most target genes,

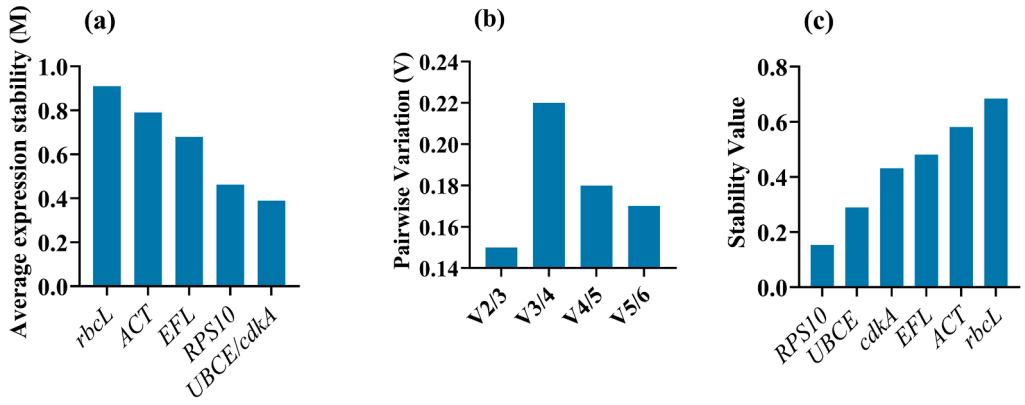

Fig. 2. Selection and stability of candidate reference genes in *Tetraselmis chui*. (a) average expression stability (M) and (b) pairwise variation (V) extrapolated from geNorm, and (c) stability value extrapolated from NormFinder. Detailed information about target genes is listed in Table 1.

especially after prolonged stress exposure (timepoint – N 48 to 72 h). A closer look at the single expression profiles over time (Fig. 3; see also supplementary material) provided insights about the regulatory starch metabolic pathways under nitrogen deprivation, with different trends during starch synthesis and degradation phases.

The reaction catalysed by AGPase is considered the primary control step for starch synthesis (Ball and Deschamps, 2009). It is also one of the main regulatory steps, with its expression peaking at the beginning of the starch synthesis phase in *O. tauri* (Sorokina et al., 2011). Previous studies on microalgae have reported that under stress conditions such as nutrient deprivation, a transient increase both in AGPase activity (Li et al., 2011; Zhu et al., 2015) and transcript amounts (Goodenough et al., 2014; Jaeger et al., 2017; Juergens et al., 2015; Li et al., 2015; Tan et al., 2016) was concurrent to the process of starch accumulation. In the present study, both *AGPLs* and *AGPSs* (the genes encoding the large and small subunit of the enzyme, respectively) were significantly down-regulated during nitrogen deprivation, while a slight increase was detected after nitrogen replenishment (Fig. 3). Transcription of these genes did not completely recover to the levels observed before stress, particularly in the case of *AGPLs,* suggesting that even if some starch was being synthesised through this pathway, anabolism was slower than catabolism. Down-regulation of AGPase activity (Yao et al., 2018) and transcription (Rismani-Yazdi et al., 2016) has been reported in microalgae under nitrogen starvation, and in *C. sorokiniana* it was demonstrated to be associated with an excessive orthophosphate presence (Zhu et al., 2015). In *T. subcordiformis*, the decline in AGPase activity during starch accumulation led to identifying a second regulatory mechanism based on SPh (Jiang et al., 2017; Yao et al., 2018). SPh in plants is involved in the last degradation steps, where it catalyses glucose phosphorylation to Glc-1-P. However, its up-regulation has been shown in connection to starch accumulation in multiple studies and species (Ikaran et al., 2015; Jaeger et al., 2017; Jiang et al., 2017; Juergens et al., 2015). The *SPh* expression profile found in this study supports a role for this gene in starch production under nitrogen deprived conditions since it exhibited an early significant increase in transcripts 24 h upon starvation and, despite being down-regulated during prolonged exposure to nutrient stress, transcript amounts remained above basal levels (Fig. 3). Interestingly, the transcriptional response to nitrogen re-supply also suggests a role for *SPh* in starch breakdown in *T. chui*, in agreement with proposed models for starch metabolism in microalgae (Busi et al., 2014; Ran et al., 2019) as a rapid up-regulation of *SPh* was observed just after 12 h.

As theoretically might be expected, most studies looking into starch pathways under nutrient stress in microalgae have detected an up-regulation of different *SSS* and *GBSS* genes during starch synthesis, especially in the early phases of stress (Blaby et al., 2013; Goodenough et al., 2014; Juergens et al., 2015; Moseley et al., 2006; Toepel et al., 2013). In the present study, several starch synthase genes (*GBSS1*, *SSS1*, *SSS2*, and *SSS5*) were up-regulated during the first 24 h of the trial (Fig. 3), coinciding with the depletion of nitrogen and with the beginning of starch storage. However, transcripts of *SSS3, SSS4* and *GBSS2* decreased during prolonged nitrogen deprivation, whereas *SSS2* was up-regulated throughout the starvation period. Such results suggest *SSS2* as a key *T. chui* isoform involved in starch synthesis under nitrogen deprivation. Toward the end of the trial (96 h after nitrogen replenishment), a recovery in transcript abundance was detected in almost all synthase genes. This final increase, observed also in other genes such as *SPh*, might represent an adaptive but transient state in response to full (or close to) recovery after the previous stressful conditions.

The cleavage of α(1–6) bonds by isoamylases is functional to structural rearrangements during both synthesis and degradation of starch. In *C. reinhardtii, ISA1* mutants are unable to produce starch and, instead, divert carbon metabolism to lipid synthesis (Kato et al., 2021). The expression of *ISA1*, *ISA2* and *ISA3* was reported to be up-regulated within 24 h from stress in *C. reinhardtii* (Juergens et al., 2015), whereas, in *C. sorokiniana*, the regulation of *ISA1* was studied over a more extended starvation period (up to 6 days), showing an increase in transcripts in parallel to degradation of starch (Li et al., 2015). In the present study, similarly to what was observed for some starch synthases, both *ISA1* and *ISA3* genes were up-regulated at the onset of starvation and subsequently down-regulated during prolonged exposure to stress (Fig. 3). The expression of both genes slowly increased during starch degradation. Thus, it was not possible to deduce a clear and direct role of *ISA1* and *ISA3* in starch metabolism according to their gene expression profiles. However, the expression of both genes slowly increased during starch degradation, suggesting both isoforms are involved throughout all starch metabolic processes.

Despite their key role in starch catabolism, amylases have been often reported to be positively regulated also in the phases of starch accumulation. For instance, an increase in transcripts encoding alpha-amylases has been reported under sulphur and phosphorus deprivation in *C. reinhardtii*, in parallel to an increase in starch content (Juergens et al., 2015; Moseley et al., 2006; Nguyen et al., 2008; Toepel et al., 2013). A transient up-regulation of several genes encoding alpha- and beta-amylases was also detected during the transition to lipid accumulation in *M. neglectum* under nitrogen deprivation, though starch content did not consequently decrease. In this study, the five AMA genes analysed exhibited an unexpected transient up-regulation after 24 h of nitrogen deprivation (Fig. 3). Then, two of them (*AMA2* and *AMA3*) showed transcript levels below starting basal levels, whereas the others returned to values close to the basal level. During the starch degradation phase, *AMA1* was the only alpha-amylase consistently up-regulated. The other genes were all down-regulated, with the exception of *AMA5*, that showed an initial transient up-regulation after 12 h of nitrogen replenishment. It has been previously stated that the existence of post-transcriptional regulatory mechanisms modulating protein abundance

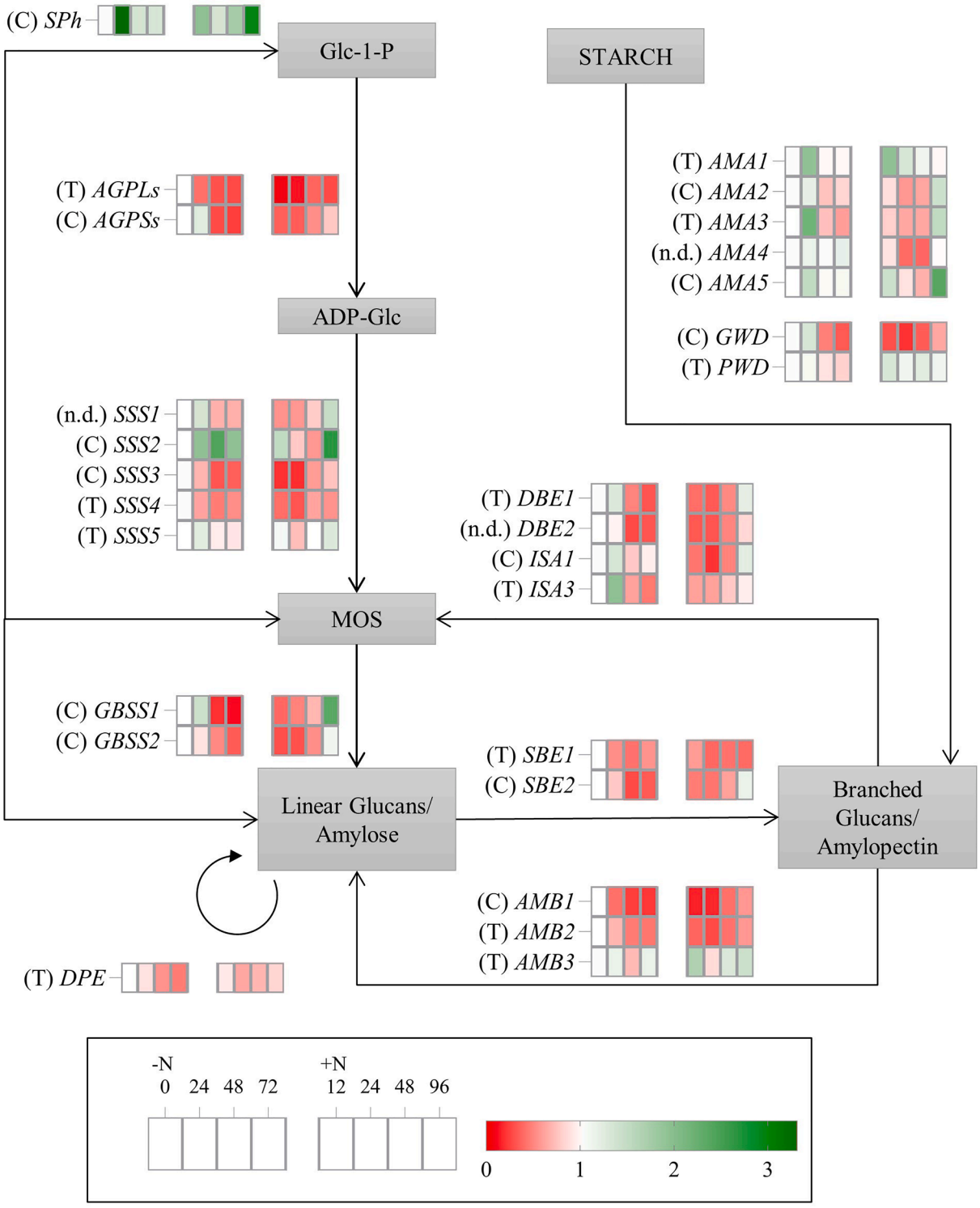

Fig. 3. Proposed regulatory model of starch synthesis and degradation pathways in *Tetraselmis chui* based on gene expression data obtained in this study. The expression profile of each gene is represented in two boxes, one for the nitrogen deprivation phase (-N, 0–72 h) and one for the recovery phase (+N, 12–96 h). Transcriptional regulation relative to timepoint zero (-N 0; white) is represented as a colour coded heat-map (Red = down-regulated, Green = up-regulated). In the genes marked with the (C) symbol, a putative chloroplast signal peptide was found in the predicted polypeptides, suggesting a putative location of the enzymes in the chloroplast. The symbol (T) indicates truncated sequence in the amino portion, and hence the analysis could not be performed, and (n.d.) indicates no signal peptide detected. The image is based on a figure by Ran et al. (2019) and Jaeger et al. (2017). Detailed information about target genes is listed in Table 1.

or enzymatic activity of amylases could explain unexpected expression profiles during starch accumulation (Jaeger et al., 2017; Nguyen et al., 2008). Moreover, it cannot be ruled out a potential role of these enzymes in cleaving glycosidic bonds during starch accumulation, which might be linked to the rearrangement of the crystal structure. As such, differential expression patterns in both alpha- and beta-amylases encoding genes have been reported concerning the starch flux during the dark/light cycle in *O. tauri* (Sorokina et al., 2011).

The role of SBE and DPE in starch metabolism has also been questioned as different expression patterns have been detected for these

enzymes during starch production in microalgae (Ran et al., 2019). Up-regulation of SBE genes has consistently been found in *C reinhardtii* during nitrogen-induced starch accumulation (Blaby et al., 2013; Goodenough et al., 2014; Juergens et al., 2015), and similar results were also observed in *D. tertiolecta* (Tan et al., 2016). However, down-regulation of *SBE2* was also observed under sulphur deprivation conditions in *C. reinhardtii* (Toepel et al., 2013). Differential expression of DPE isoforms was instead observed under nitrogen stress in *C. reinhardtii*, with *DPE1* being down-regulated after 24 h of stress, whereas *DPE2* transcripts increased (Juergens et al., 2015). In the present study, *SBE1, SBE2* and *DPE* were all significantly down-regulated during the starvation phase (Fig. 3). Once nitrogen was resupplied in the medium, *DPE* transcripts almost returned to basal levels, whereas *SBE1* and *SBE2* remained down-regulated. This somewhat unexpected result could be explained either by the presence of additional isoforms being active in this process or by post-transcriptional regulatory mechanisms that could play a role in the regulation of these genes, as suggested for isoamylases or amylases encoding genes (Ikaran et al., 2015; Jaeger et al., 2017; Nguyen et al., 2008).

Compared to most starch-related genes included in the present study, regulation under stress conditions of PWD and GWD has been tackled much less in scientific literature. In *C. reinhardtii*, two different *GWD* genes and *PWD* were down-regulated under nitrogen starvation 24 h after the onset of stress, when starch content was increasing (Juergens et al., 2015). In contrast, in the green microalga *M. neglectum*, three *GWD* genes exhibited a significant up-regulation in nitrogen-deprived cells after 24 h of stress when starch content peaked, whereas *PWD* remained stable. Moreover, during the recovery phase after nitrogen resupply, transcript levels of *GWD* were unaffected, whereas those of *PWD* genes were down-regulated and returned to basal levels (Jaeger et al., 2017). In the present study, the expression of *GWD* exhibited an up-regulation at the beginning of the starvation phase (Fig. 3). Still, it was then strongly repressed after 48 h and onto the starch degradation phase. However, *PWD* remained relatively stable throughout the trial, with transcript amounts slightly decreasing under nitrogen starvation but increasing after nitrogen replenishment. Altogether, these findings reveal significant differences in the transcriptional regulation of WD in microalgae and potentially suggest phosphorylation of glucan chains as a process occurring in all stages of starch metabolism. In support of this idea, in the *O. tauri* day-night cycle model, *PWD* was shown to have a 12 h circadian rhythm. Expression peaks were thus observed both in the middle of daylight and night-time, potentially underpinning the importance of this enzyme in starch anabolism and catabolism (Sorokina et al., 2011).

As a whole, findings obtained in this study suggest firstly that the green microalga *T. chui* displays species-specific transcriptional regulatory pathways in starch metabolism. This is in agreement with a recent review showing that the expression of starch-related genes during stress differs greatly between species and conditions and that the activity of typical anabolic enzymes can be detected during catabolism and vice versa (Ran et al., 2019). Secondly, the up-regulation of degrading enzymes during starch production in this study, as similarly reported in multiple species (Nguyen et al., 2008; Zhang et al., 2004; Ikaran et al., 2015), supports the hypothesis that catabolic enzymes may play a role in maintaining an active flux of substrates in the starch biosynthetic pathway (Moseley et al., 2006). In this regard, the expression profile of *SPh* detected in *T. chui* suggests a potential role of this enzyme in starch synthesis, in agreement with the results of a former study performed on *T. subcordiformis* (Jiang et al., 2017). Finally, the results of this study allow to formulate the hypothesis that post-transcriptional regulatory mechanisms may play a critical role in starch metabolism in *T. chuii*, as was formerly suggested for other species (Nguyen et al., 2008; Ikaran et al., 2015; Jaeger et al. 2017). Further studies could explore this route, possibly using "-omics" technologies to better understand and characterise the accumulation of reserve starch in this industrially relevant species.

4. Conclusions

T. chui proved to be an efficient and fast starch producer under nitrogen deprivation in the pilot-scale trial here conducted, with a maximum relative content of 59% storage starch. A full recovery was achieved between 48 and 96 h after nitrogen replenishment, with a speedy degradation of starch and an upturn of photosynthetic activity. However, no clear relationships between evolution of starch content and expression profiles of target genes involved in starch metabolism could be established during starch synthesis and degradation phases, which strongly suggest that specific post-transcriptional regulatory mechanisms may play a crucial role in starch metabolism in *T. chui*.

5. Data availability

Data available from authors.

CRediT authorship contribution statement

Giorgia Carnovale: Conceptualization, Investigation, Writing – original draft, Visualization. **Carmen Lama:** Investigation, Formal analysis. **Sonia Torres:** Investigation, Formal analysis. **Filipa Rosa:** Investigation, Writing – review & editing. **Lalia Mantecón:** Conceptualization, Supervision. **Svein Jarle Horn:** Supervision, Writing – review & editing. **Kari Skjånes:** Conceptualization, Supervision, Writing – review & editing, Resources, Project administration, Funding acquisition. **Carlos Infante:** Conceptualization, Investigation, Writing – original draft, Resources, Formal analysis.

Declaration of Competing Interest

The authors declare that they have no known competing financial interests or personal relationships that could have appeared to influence the work reported in this paper.

Acknowledgments

This work received financial support from Research Council Norway ('ALGAE TO FUTURE' project #267872) and NordForsk ('NordAqua' project #82845). We thank Stig A. Borgvang at NIBIO for funding acquisition and coordination of the ALGAE TO FUTURE project, Ksenia Gulyaeva for her support with ion chromatography and Hanne Skomedal for supporting and managing the NIBIO team.

Appendix A. Supplementary data

Supplementary data to this article can be found online at https://doi.org/10.1016/j.biortech.2022.127222.

References

Andersen, C.L., Jensen, J.L., Ørntoft, T.F., 2004. Normalization of real-time quantitative reverse transcription-PCR data: a model-based variance estimation approach to identify genes suited for normalization, applied to bladder and colon cancer data sets. Cancer Res. 64, 5245–5250. https://doi.org/10.1158/0008-5472.CAN-04-0496.

Armenteros, J.J.A., Salvatore, M., Emanuelsson, O., Winther, O., Von Heijne, G., Elofsson, A., Nielsen, H., 2019. Detecting sequence signals in targeting peptides using deep learning. Life Sci. Alliance 2 (5), e201900429. https://doi.org/10.26508/LSA.201900429.

Ball, S.G., Deschamps, P., 2009. Chapter 1 – Starch Metabolism. In: Harris, E.H., Stern, D. B., Witman, G.B. (Eds.), The *Chlamydomonas* Sourcebook. Academic Press, London, pp. 1–40.

Blaby, I.K., Glaesener, A.G., Mettler, T., Fitz-Gibbon, S.T., Gallaher, S.D., Liu, B., Boyle, N.R., Kropat, J., Stitt, M., Johnson, S., Benning, C., Pellegrini, M., Casero, D., Merchant, S.S., 2013. Systems-level analysis of nitrogen starvation-induced modifications of carbon metabolism in a *Chlamydomonas reinhardtii* starchless mutant. Plant Cell 25, 4305–4323. https://doi.org/10.1105/tpc.113.117580.

Brányiková, I., Maršálková, B., Doucha, J., Brányik, T., Bišová, K., Zachleder, V., Vítová, M., 2011. Microalgae-novel highly efficient starch producers. Biotechnol. Bioeng. 108, 766–776. https://doi.org/10.1002/bit.23016.
Busi, M.V., Barchiesi, J., Martín, M., Gomez-Casati, D.F., 2014. Starch metabolism in green algae. Starch - Stärke 66, 28–40. https://doi.org/10.1002/star.201200211.
Cao, S., Zhang, X., Ye, N., Fan, X., Mou, S., Xu, D., Liang, C., Wang, Y., Wang, W., 2012. Evaluation of putative internal reference genes for gene expression normalization in *Nannochloropsis sp*. by quantitative real-time RT-PCR. Biochem. Biophys. Res. Commun. 424, 118–123. https://doi.org/10.1016/j.bbrc.2012.06.086.
Carnovale, G., Rosa, F., Shapaval, V., Dzurendova, S., Kohler, A., Wicklund, T., Horn, S. J., Barbosa, M.J., Skjånes, K., 2021. Starch rich *Chlorella vulgaris*: high-throughput screening and up-scale for tailored biomass production. Appl. Sci. 11, 9025. https://doi.org/10.3390/app11199025.
Chapman, J.R., Waldenström, J., 2015. With reference to reference genes: a systematic review of endogenous controls in gene expression studies. PLoS ONE 10 (11), e0141853. https://doi.org/10.1371/journal.pone.0141853.
Chowdhury, H., Loganathan, B., 2019. Third-generation biofuels from microalgae: a review. Curr. Opin. Green Sustain. Chem. 20, 39–44. https://doi.org/10.1016/j.cogsc.2019.09.003.
Corteggiani Carpinelli, E., Telatin, A., Vitulo, N., Forcato, C., D'Angelo, M., Schiavon, R., Vezzi, A., Giacometti, G.M., Morosinotto, T., Valle, G., 2014. Chromosome scale genome assembly and transcriptome profiling of *Nannochloropsis gaditana* in nitrogen depletion. Mol. Plant 7, 323–335. https://doi.org/10.1093/MP/SST120.
Gao, P., Wang, J., Wen, J., Woloschak, G.E., 2020. Selection of reference genes for tissue/organ samples of adults of *Eucryptorrhynchus scrobiculatus*. PLoS ONE 15 (2), e0228308. https://doi.org/10.1371/journal.pone.0228308.
Gifuni, I., Olivieri, G., Krauss, I.R., D'Errico, G., Pollio, A., Marzocchella, A., 2017. Microalgae as new sources of starch: Isolation and characterization of microalgal starch granules. Chem. Eng. Trans. 57, 1423–1428. https://doi.org/10.3303/CET1757238.
Goodenough, U., Blaby, I., Casero, D., Gallaher, S.D., Goodson, C., Johnson, S., Lee, J.H., Merchant, S.S., Pellegrini, M., Roth, R., Rusch, J., Singh, M., Umen, J.G., Weiss, T.L., Wulan, T., 2014. The path to triacylglyceride obesity in the sta6 strain of *Chlamydomonas reinhardtii*. Eukaryot. Cell 13, 591–613. https://doi.org/10.1128/EC.00013-14.
Guo, R., Lee, M.A., Ki, J.S., 2013. Normalization genes for mRNA expression in the marine diatom *Ditylum brightwellii* following exposure to thermal and toxic chemical stresses. J. Appl. Phycol. 25, 1101–1109. https://doi.org/10.1007/s10811-012-9908-z.
Ikaran, Z., Suárez-Alvarez, S., Urreta, I., Castañón, S., 2015. The effect of nitrogen limitation on the physiology and metabolism of *Chlorella vulgaris* var L3. Algal Res. 10, 134–144. https://doi.org/10.1016/j.algal.2015.04.023.
Jaeger, D., Winkler, A., Mussgnug, J.H., Kalinowski, J., Goesmann, A., Kruse, O., 2017. Time-resolved transcriptome analysis and lipid pathway reconstruction of the oleaginous green microalga *Monoraphidium neglectum* reveal a model for triacylglycerol and lipid hyperaccumulation. Biotechnol. Biofuels 10, 1–35. https://doi.org/10.1186/s13068-017-0882-1.
Janssen, J.H., Driessen, J.L.S.P., Lamers, P.P., Wijffels, R.H., Barbosa, M.J., 2018. Effect of initial biomass-specific photon supply rate on fatty acid accumulation in nitrogen depleted *Nannochloropsis gaditana* under simulated outdoor light conditions. Algal Res. 35, 595–601. https://doi.org/10.1016/j.algal.2018.10.002.
Jiang, J., Yao, C., Cao, X., Liu, Y., Xue, S., 2017. Characterization of starch phosphorylase from the marine green microalga (*Chlorophyta*) *Tetraselmis subcordiformis* reveals its potential role in starch biosynthesis. J. Plant Physiol. 218, 84–93. https://doi.org/10.1016/j.jplph.2017.07.019.
Juergens, M.T., Deshpande, R.R., Lucker, B.F., Park, J.J., Wang, H., Gargouri, M., Omar Holguin, F., Disbrow, B., Schaub, T., Skepper, J.N., Kramer, D.M., Gang, D.R., Hicks, L.M., Shachar-Hill, Y., 2015. The regulation of photosynthetic structure and function during nitrogen deprivation in *Chlamydomonas reinhardtii*. Plant Physiol. 167, 558–573. https://doi.org/10.1104/pp.114.250530.
Kato, Y., Oyama, T., Inokuma, K., Vavricka, C.J., Matsuda, M., Hidese, R., Satoh, K., Oono, Y., Chang, J.-S., Hasunuma, T., Kondo, A., 2021. Enhancing carbohydrate repartitioning into lipid and carotenoid by disruption of microalgae starch debranching enzyme. Commun. Biol. 4, 450. https://doi.org/10.1038/s42003-021-01976-8.
Koski, L.B., Gray, M.W., Lang, B.F., Burger, G., 2005. AutoFACT: An Auto matic F unctional A nnotation and C lassification T ool. BMC Bioinf. 6, 151. https://doi.org/10.1186/1471-2105-6-151.
Lauritano, C., De Luca, D., Amoroso, M., Benfatto, S., Maestri, S., Racioppi, C., Esposito, F., Ianora, A., 2019. New molecular insights on the response of the green alga *Tetraselmis suecica* to nitrogen starvation. Sci. Rep. 9, 1–12. https://doi.org/10.1038/s41598-019-39860-5.
Li, L., Zhang, G., Wang, Q., 2016. De novo transcriptomic analysis of *Chlorella sorokiniana* reveals differential genes expression in photosynthetic carbon fixation and lipid production. BMC Microbiol. 16, 1–12. https://doi.org/10.1186/S12866-016-0839-8/FIGURES/6.
Li, T., Gargouri, M., Feng, J., Park, J.J., Gao, D., Miao, C., Dong, T., Gang, D.R., Chen, S., 2015. Regulation of starch and lipid accumulation in a microalga *Chlorella sorokiniana*. Bioresour. Technol. 180, 250–257. https://doi.org/10.1016/j.biortech.2015.01.005.
Li, Y., Han, D., Sommerfeld, M., Hu, Q., 2011. Photosynthetic carbon partitioning and lipid production in the oleaginous microalga *Pseudochlorococcum sp*. (*Chlorophyceae*) under nitrogen-limited conditions. Bioresour. Technol. 102, 123–129. https://doi.org/10.1016/j.biortech.2010.06.036.
Lim, D.K.Y., Schuhmann, H., Thomas-Hall, S.R., Chan, K.C.K., Wass, T.J., Aguilera, F., Adarme-Vega, T.C., Dal'Molin, C.G.O., Thorpe, G.J., Batley, J., Edwards, D., Schenk, P.M., 2017. RNA-Seq and metabolic flux analysis of *Tetraselmis sp*. M8 during nitrogen starvation reveals a two-stage lipid accumulation mechanism. Bioresour. Technol. 244, 1281–1293. https://doi.org/10.1016/J.BIORTECH.2017.06.003.
Liu, Q., Xing, Y., Li, Y., Wang, H., Mi, T., Zhen, Y.u., Yu, Z., Lin, S., 2020. Carbon fixation gene expression in *Skeletonema marinoi* in nitrogen-, phosphate-, silicate-starvation, and low-temperature stress exposure. J. Phycol. 56 (2), 310–323. https://doi.org/10.1111/JPY.12936.
Livak, K.J., Schmittgen, T.D., 2001. Analysis of Relative Gene Expression Data Using Real-Time Quantitative PCR and the 2−ΔΔCT Method. Methods 25, 402–408. https://doi.org/10.1006/meth.2001.1262.
Mantecón, L., Moyano, R., Cameán, A.M., Jos, A., 2019. Safety assessment of a lyophilized biomass of *Tetraselmis chuii* (TetraSOD®) in a 90 day feeding study. Food Chem. Toxicol. 133, 110810 https://doi.org/10.1016/j.fct.2019.110810.
Moseley, J.L., Chang, C.W., Grossman, A.R., 2006. Genome-based approaches to understanding phosphorus deprivation responses and PSR1 control in *Chlamydomonas reinhardtii*. Eukaryot. Cell 5, 26–44. https://doi.org/10.1128/EC.5.1.26-44.2006.
Mou, S., Zhang, X., Miao, J., Zheng, Z., Xu, D., Ye, N., 2015. Reference genes for gene expression normalization in *Chlamydomonas sp*. ICE-L by quantitative real-time RT-PCR. J. Plant Biochem. Biotechnol. 24, 276–282. https://doi.org/10.1007/s13562-014-0268-4.
Nguyen, A.V., Thomas-Hall, S.R., Malnoë, A., Timmins, M., Mussgnug, J.H., Rupprecht, J., Kruse, O., Hankamer, B., Schenk, P.M., 2008. Transcriptome for photobiological hydrogen production induced by sulfur deprivation in the green alga *Chlamydomonas reinhardtii*. Eukaryot. Cell 7, 1965–1979. https://doi.org/10.1128/EC.00418-07.
Patelou, M., Infante, C., Dardelle, F., Randewig, D., Kouri, E.D., Udvardi, M.K., Tsiplakou, E., Mantecón, L., Flemetakis, E., 2020. Transcriptomic and metabolomic adaptation of *Nannochloropsis gaditana* grown under different light regimes. Algal Res. 45, 101735 https://doi.org/10.1016/J.ALGAL.2019.101735.
Radonić, A., Thulke, S., Mackay, I.M., Landt, O., Siegert, W., Nitsche, A., 2004. Guideline to reference gene selection for quantitative real-time PCR. Biochem. Biophys. Res. Commun. 313, 856–862. https://doi.org/10.1016/j.bbrc.2003.11.177.
Ran, W., Wang, H., Liu, Y., Qi, M., Xiang, Q., Yao, C., Zhang, Y., Lan, X., 2019. Storage of starch and lipids in microalgae: Biosynthesis and manipulation by nutrients. Bioresour. Technol. 291, 121894 https://doi.org/10.1016/j.biortech.2019.121894.
Reitan, K.I., Øie, G., Jørgensen, H., Wang, X., 2021. Chemical composition of selected marine microalgae, with emphasis on lipid and carbohydrate production for potential use as feed resources. J. Appl. Phycol. 33, 3831–3842. https://doi.org/10.1007/s10811-021-02586-x.
Rismani-Yazdi, H., Haznedaroglu, B.Z., Hsin, C., Peccia, J., 2016. Transcriptomic analysis of the oleaginous microalga *Neochloris oleoabundans* reveals metabolic insights into triacylglyceride accumulation. Adv. Biofuel Prod. Algae Aquat. Plants 325–357. https://doi.org/10.1201/b16341-20.
Scarsini, M., Thiriet-Rupert, S., Veidl, B., Mondeguer, F., Hu, H., Marchand, J., Schoefs, B., 2022. The transition toward nitrogen deprivation in diatoms requires chloroplast stand-by an deep metabolic reshuffling. Front. Plant Sci. 12, 760516 https://doi.org/10.3389/FPLS.2021.760516/FULL.
Shahid, A., Khan, F., Ahmad, N., Farooq, M., Mehmood, M.A., 2020. Chapter 14 - Microalgal Carbohydrates and Proteins: Synthesis, Extraction, Applications, and Challenges. In: Alam, M.A., Xu, J.L., Wang, Z. (Eds.), Microalgae Biotechnology for Food, Health and High Value Products. Springer Singapore, Singapore, pp. 433–468.
Sorokina, O., Corellou, F., Dauvillée, D., Sorokin, A., Goryanin, I., Ball, S., Bouget, F.-Y., Millar, A.J., 2011. Microarray data can predict diurnal changes of starch content in the picoalga *Ostreococcus*. BMC Syst. Biol. 5, 36. https://doi.org/10.1186/1752-0509-5-36.
Tan, K.W.M., Lin, H., Shen, H., Lee, Y.K., 2016. Nitrogen-induced metabolic changes and molecular determinants of carbon allocation in *Dunaliella tertiolecta*. Sci. Rep. 6, 1–13. https://doi.org/10.1038/srep37235.
Toepel, J., Illmer-Kephalides, M., Jaenicke, S., Straube, J., May, P., Goesmann, A., Kruse, O., 2013. New insights into *Chlamydomonas reinhardtii* hydrogen production processes by combined microarray/RNA-seq transcriptomics. Plant Biotechnol. J. 11, 717–733. https://doi.org/10.1111/pbi.12062.
Torres, S., Lama, C., Mantecón, L., Flemetakis, E., Infante, C., Wu, S.-B., 2021. Selection and validation of reference genes for quantitative real-time PCR in the green microalgae *Tetraselmis chui*. PLoS ONE 16 (1), e0245495. https://doi.org/10.1371/journal.pone.0245495.
Vandesompele, J., De Preter, K., Pattyn, F., Poppe, B., Van Roy, N., De Paepe, A., Speleman, F., 2002. Accurate normalization of real-time quantitative RT-PCR data by geometric averaging of multiple internal control genes. Genome Biol. 3 https://doi.org/10.1186/gb-2002-3-7-research0034.
Yao, C., Ai, J., Cao, X., Xue, S., Zhang, W., 2012. Enhancing starch production of a marine green microalga *Tetraselmis subcordiformis* through nutrient limitation. Bioresour. Technol. 118, 438–444. https://doi.org/10.1016/j.biortech.2012.05.030.
Yao, C., Chu, Y., Liu, Y., Cao, X., 2017. Photosynthetic performance in relation to nitrogen limitation-induced starch production in a marine green microalga *Tetraselmis subcordiformis*. Res. Rev. J. Bot. Sci. 6, 57–63.
Yao, C., Jiang, J., Cao, X., Liu, Y., Xue, S., Zhang, Y., 2018. Phosphorus enhances photosynthetic storage starch production in a green microalga (Chlorophyta) *Tetraselmis subcordiformis* in nitrogen starvation conditions. J. Agric. Food Chem. 66, 10777–10787. https://doi.org/10.1021/acs.jafc.8b04798.
Zhang, C., Li, S., Ho, S.H., 2021. Converting nitrogen and phosphorus wastewater into bioenergy using microalgae-bacteria consortia: A critical review. Bioresour. Technol. 342, 126056 https://doi.org/10.1016/J.BIORTECH.2021.126056.

Zhang, Z., Shrager, J., Jain, M., Chang, C.W., Vallon, O., Grossman, A.R., 2004. Insights into the survival of *Chlamydomonas reinhardtii* during sulfur starvation based on microarray analysis of gene expression. Eukaryot. Cell 3 (5), 1331–1348. https://doi.org/10.1128/EC.3.5.1331-1348.2004.

Zhu, S., Wang, Y., Xu, J., Shang, C., Wang, Z., Xu, J., Yuan, Z., 2015. Luxury uptake of phosphorus changes the accumulation of starch and lipid in *Chlorella sp*. under nitrogen depletion. Bioresour. Technol. 198, 165–171. https://doi.org/10.1016/j.biortech.2015.08.142.

https://www.imicrobe.us/ (accessed 28/03/2022).